Journal Pre-proof

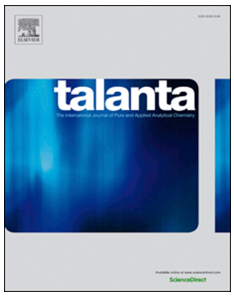

Sensitive measurement of tumor markers somatostatin receptors using an octreotide-directed Pt nano-flakes driven electrochemical sensor

Cong Cong, Kexin Bian, Xuwu Zhang, Liyao Luo, Lei Li, Hongyu He, Chunhui Li, Qianqian Zhao, Shuai Wang, Zining Hao, Yaqian He, Dawei Gao

PII: S0039-9140(19)30919-1

DOI: https://doi.org/10.1016/j.talanta.2019.120286

Reference: TAL 120286

To appear in: *Talanta*

Received Date: 11 May 2019

Revised Date: 15 August 2019

Accepted Date: 20 August 2019

Please cite this article as: C. Cong, K. Bian, X. Zhang, L. Luo, L. Li, H. He, C. Li, Q. Zhao, S. Wang, Z. Hao, Y. He, D. Gao, Sensitive measurement of tumor markers somatostatin receptors using an octreotide-directed Pt nano-flakes driven electrochemical sensor, *Talanta* (2019), doi: https://doi.org/10.1016/j.talanta.2019.120286.

Graphical Abstract

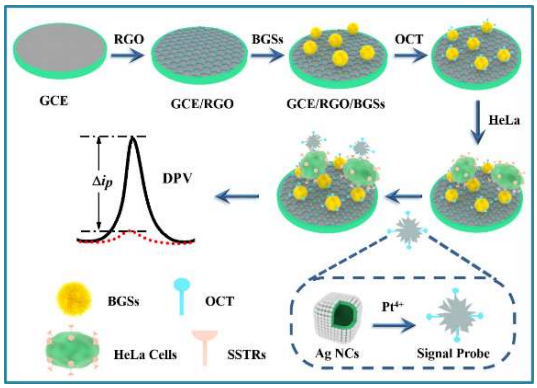

SYNOPSIS: An ultrasensitive sandwich electrochemical biosensor was used for detection of tumor-specific markers to evaluate tumor cells.

Sensitive Measurement of Tumor Markers Somatostatin Receptors Using an Octreotide-Directed Pt Nano-Flakes Driven Electrochemical Sensor

Cong Cong [†,‡,#], Kexin Bian[†,#], Xuwu Zhang[†,‡], Liyao Luo[†], Lei Li[†], Hongyu He[†], Chunhui Li[†], Qianqian Zhao[†], Shuai Wang[†], Zining Hao[†], Yaqian He[†], Dawei Gao[*,†,‡,§]

[†]Applying Chemistry Key Lab of Hebei Province, Department of Bioengineer, Yanshan University, No.438 Hebei Street, Qinhuangdao, 066004, China.

[‡]State Key Laboratory of Metastable Materials Science and Technology, Yanshan University, Qinhuangdao 066004, P. R. China.

[§]Hebei Province Asparagus Industry Technology Research Institute, Qinhuangdao, P. R. China.

[*]Corresponding author: Prof. Dawei Gao, Tel: (+86)13930338376.

E-mail: dwgao@ysu.edu.cn

[#]Cong Cong and Kexin Bian contributed equally to this work.

ABSTRACT: Tumor markers play an important role in the early diagnosis and therapeutic effect monitoring of tumors. An electrochemical biosensor was developed based on multi-branched gold nanoshells (BGSs) and octreotide (OCT) functionalized Pt nano-flakes (PtNFs) modified electrodes, which was used for detection of tumor-specific markers to evaluate tumor cells. Sandwich-type nano-hybrid materials were prepared by layer-by-layer modification. First, reduced graphene oxide (RGO) and BGSs were modified as electronic materials onto glassy carbon electrodes (GCE). This modified electrode has strong electron transfer capability and large electrode surface area. The OCT was then anchored to the surface of BGSs to sensitively detect Somatostatin receptors (SSTRs) on the surface of HeLa cells. In addition, PtNFs were synthesized using a dual-template method, and OCT template on the surface of PtNFs, as an adsorption bioprobe, was used to reduce the H_2O_2 and amplify the electrochemical signal of biosensor. The proposed biosensor can be applied to the quantitative broad linear range of HeLa cells covering from 10 to 1×10^6 cells mL^{-1} (R^2=0.9998) and the limit of detection (LOD) was 2 cells mL^{-1}. The experimental results also show that the sensor has good stability, biocompatibility and high selectivity, which has great potential for clinical application.

KEYWORDS: Tumor markers, Eletrochemical sensor, Pt nano-flakes,

Somatostatin receptors

Introduction

Precise detection of biomarkers is vital for the early diagnosis and therapeutic effect monitoring of tumors.[1-3] SSTRs are overexpressed on the surface of various tumor cells such as neuroendocrine tumors, breast cancer, prostate cancer, and cervical cancer.[4-6] Therefore, the expression of SSTRs can be used as a broad-spectrum biomarker in evaluating the therapeutic effects and early prediction for many types of cancer. It is necessary to develop high selectivity, super sensitive methods for studying real-time biological markers for tumor detection.

Ligand-based electrochemical biosensor, which requires no labeling and enable high receptor sensitivity, is an important cell-based method by detecting biomarkers.[7] Ligand is a kind of specific and affinity molecule that can recognizes and interacts with anchor protein.[8] OCT is one of the most widely studied somatostatin (SST) analogues, and its affinity for SSTRs is 70 times comparing with that of SST.[9] Therefore, detection of tumor cells based on specific binding of OCT and SSTRs is a worthwhile strategy. However, it is necessary for the detection of biomarkers to require a high precision, which is a major obstacle to tumor cell detection at present. Therefore, to achieve the purpose of detection by amplifying the response signal, and committed to the development of some highly selective ultra-sensitive electrochemical biosensors has become crucial.

With the rapid development of nanotechnology, various nanomaterials have been widely applied in the development of electrochemical biosensors for the

enhancement of sensor sensitivity and signal amplification.[10] As an isolated two-dimensional carbon nanomaterial, RGO has attracted extensive attention in the field of electrochemical biosensors due to its high electron conductivity, large specific surface area, fast heterogeneous electron transfer rate at the edge of RGO sheet.[11-13] RGO also is served as a strong support for nanoparticles to form hybrid materials with better properties.[14, 15] RGO modified with gold nanomaterials can provide the current response of the modified electrode, have good conductivity, and afford abundant binding sites for subsequent biological molecules.[16] In addition, the combination of biological molecules and nanomaterials has also shown great potentials for development in electrochemical biosensor interfaces. Various metals and metal oxide nanomaterials can be developed into sensitive electrochemical biosensors as electrocatalysts, such as Au, Pt and Pd.[17] Among them, Pt nanoparticles, especially two-dimensional structures, have better electrocatalytic properties, excellent biocompatibility and large specific surface area,[18-20] which can be used for preparing various biosensors.

Inspired by these, this study designed a novel electrochemical sensor for ultrasensitive detection, which can be used to evaluate the number of tumor cells based on the specific detection of biomarkers SSTRs (Scheme 1). OCT, as a hydrosoluble polypeptide, containing amines amidogen, and a hydroxyl disulfide bond, which is liable to combine with ions. PtNFs were assembled with dual-template method, which was that activating chemical groups of the OCT template to direct the synthesis of Ag nanocubes as sacrificial metal, and then

sacrificial template was used to guide the synthesis of the PtNFs. As electronic materials, RGO and BGSs were modified on GCE to improve the ability of electrons transfer to the electrode surface. On the other hand, it increased the surface area of the electrode and modified more biological molecules to amplify the signal. The OCT was then respectively anchored on the surface of BGSs to detect SSTRs on the surface of HeLa cells. In addition, the OCT on the surface of PtNFs forming an adsorption bioprobe, which can also be used to reduce H_2O_2 and amplify the electrochemical signal of the biosensor.

EXPERIMENTAL

Materials. Octreotide (OCT, GL Biochem Ltd., Shanghai, China), $AgNO_3$ (North Fine Chemicals Co., Ltd., Beijing, China), sodium borohydride ($NaBH_4$, Tianjin Guangfu Fine Chemical Research Institute, Tianjin, China), ascorbic acid (AA, Beijing Biodee Biotechnology Co., Ltd., Beijing, China), potassium hydroxide (KOH, Sinopharm Chemical Reagent Co., Ltd., Shanghai, China), hydrogen chloride (HCl, Tianjin Fengchuan Chemical Reagent Technologies Co., Ltd., Tianjin, China), auric chloride ($AuCl_3$, Xiya Chemical Co., Ltd., Chengdu, China), absolute ethyl alcohol (C_2H_5OH, Tianjin Jindongtianzheng Fine Chemical Reagent Co., Ltd., Tianjin, China), platinum chloride ($PtCl_4$, Xiya Chemical Co., Ltd., Jinan, China) and commercial palladium on carbon (Pd/C, 20 wt %, Sigma-Aldrich, Inc.) catalyst were used in this work. All solvents and chemicals are analytical grade and are used without further purification and ultrapure water (18.2 MΩ/cm) was used throughout the experiment.

Characterization methods. The morphologies and particle sizes of the samples were determined using model Transmission electron microscope (TEM) operated at 80 kV accelerating voltage. TEM samples were prepared by placing drops of the AgNCs/PtNFs suspension onto carbon-coated copper grids. The chemical compositions of the samples were analyzed by Energy dispersive spectroscopy (EDS), which was carried out on an X-ray spectrometer (Oxford Link-ISIS) instrument operated at 200 kV. X-Ray diffraction (XRD) was employed to examine the structure and crystallographic nature of the materials, which was freeze-dried into powder in advance. It was carried on JEM-2010 instrument operated at an accelerating voltage of 200 kV. Absorption spectra were observed by Ultraviolet–visible spectrophotometer (UV–vis, SHIMADZU UV2550, Japan) to further verify loading capacity and mechanism. Malvern Zetasizer ZS (Malvern Instruments, UK) was used to assess the sizes and surface zeta potentials of the prepared PtNFs to measure the stability and the charged condition. The characteristic spectrum was obtained by Fourier transform infrared spectroscopy to analyze its structural characteristics. All electrochemical measurements were performed in an electrochemical workstation (CHI-660E, Shanghai, China) with a conventional three component electrochemical cell, including a modified glassy carbon electrode (GCE) as the working electrode, a KCl-saturated calomel electrode as the reference electrode, and a platinum foil as the counter electrode. Electrochemical impedance spectroscopy (EIS), Cyclic

voltammetry (CV) and differential pulse voltammetry (DPV) measurements for characterization of the interface properties of the modified electrode.

Synthesis of Ag nanocubes. Ag nanocubes (AgNCs) were synthesized based on OCT as templated for bio-mineralization of silver.[21] In short, 200 μL OCT solution (0.25 mM, pH 2.2) as placed at 80°C metal bath for 20 min. After cooled at room temperature, the solution was mixed with 63 μL AA (7 mg mL^{-1}) and 327 μL $AgNO_3$ (3.5 mM) followed by incubation at room temperature for 24 h. Subsequently, 100 μL of a freshly prepared $NaBH_4$ solution (15 mM) was injected into the above incubated solution. The reaction product was centrifuged (8000 rpm, 15 min), and washed twice to obtain a dispersion of AgNCs.

Synthesis of Pt nano-flakes. 2 mL $PtCl_4$ solution (2 mM) and synthesized Ag NCs were mixed uniformly vigorous magnetic stirring for 15 min. Subsequently, 1 mL AA solution (40 mM) was injected into the above solution incubating for 10 min to promote the Pt crystal growth, then the reduction reaction was triggered by rapid injection of 30 μL of $NaBH_4$ (50 mM). When the solution turned to dark blue, the PtNFs were successfully synthesized under gentle shaking. Finally, the obtained Pt nano-flakes (PtNFs) were collected through 3 cycles of centrifugation/resuspension in water.

Synthesis of the branched gold nanoshells. BGSs were synthesized by dual-template cascade mothed previously described.[22] The AgNCs and the gold precursor ($AuCl_3$) were thoroughly mixed to trigger the displacement reaction, and then the $AuCl_3$ solution and reductant were added to the mixture to promote

the crystal growth. Finally, the formation of dendritic structures, which grew on the surface of BGSs, were driven by reduction of gold chloride to high energy crystal faces of gold species.

Construction of electrochemical biosensors and detection. GCE was modified using the reported BGSs as an electronic conduction enhancement, and a series of electrochemical experiments were used to detect its excellent specific surface area and predict its application potentials.

The GCE (diameter 3 mm) was polished to the mirror surface by polishing powder with particle sizes 1.0, 0.3 and 0.05 μm (Al_2O_3), followed by rinsing with deionized water and C_2H_5OH. To evaluate the electrical conductivity of BGSs and the electrocatalytic performance of PtNFs, 5 μL nanoparticle suspension droplets were placed on the surface of GCE after pretreatment and left to dry overnight.

For the preparation of the electrode modified by RGO/BGSs/OCT, 5 μL oxidized RGO suspension and 5 μL BGSs solution were successively applied to dry GCE at room temperature for 3 h after polishing treatment, and then 5 μL OCT solution with concentration of 0.5 mM was applied to the electrode surface at room temperature for 1 h and then cleaned with deionized water to remove residual free polypeptide molecules. The electrochemical test conditions for the electrode modified by BGSs were KCl electrolyte with a concentration of 5 mM $[Fe(CN)_6]^{-3/-4}$ and a concentration of 0.1 M, with a sweep rate of 50 mV/s.

In order to construct a sandwich-type electrochemical biosensor, the modified electrode was incubated in HeLa cells of different concentrations for 1 h in 37° C

environment. Electrode-to-cell capture is due to the ability of OCT to bind to SSTRs of tumors. The incubated electrode was carefully rinsed with PBS buffer to remove uncaptured HeLa cells, and then the cells were incubated with 10 μL of the PtNFs signal probes for another 1 h at 37°C, followed by careful washing with PBS to remove unbound signal probes. Finally, the electrochemical sensor was measured by DPV. The electrolyte was a 0.01 M PBS solution with a potential range from 0 to 0.5 V. All of the measurements were repeated three times at 37° C and all electrolytes were bubbled with nitrogen for 30 min before use.

Biocompatibility of the electrochemical devices. Biosafety of biosensor should be considered first in medicine applications, therefore, the biological compatibility of was evaluated using live/dead cell staining experiments with fluorescein diacetate (FDA). Cell activity was detected through the standard 3-(4,5-dimethylthiazol-2-yl)-2,5-diphenyltetrazolium bromide (MTT) assay.

RESULTS AND DISCUSSION

Material characterizations of PtNFs. The synthesis of PtNFs was based on an electrochemical displacement reaction between Pt and Ag, AgNCs acting as a sacrificial template. To prepare PtNPs, the AgNCs, $PtCl_4$ (precursor solution) and AA (mild reducing agent) were uniformly mixed, followed by injection of freshly prepared sodium borohydride (strong reducing agent). In our study, uniform nucleation was produced by a rapid injection of strong reducing agent $NaBH_4$ into the precursors solution of metal ions to reduce the Pt ion precursor and produce explosive nucleation. Furtherly, remaining Pt ion precursor was reduced gradually by injecting AA solution, simultaneously, the Pt atoms generated were preferentially grown on the high-energy crystal surface that was not selectively bound by polypeptide and AgCl.[18]

The TEM images show the structural morphologies of the prepared AgNCs and PtNFs samples, and the visual morphology of the AgNCs were revealed in the SEM images. It's worth noting that peptides could be used to direct the growth of nanoparticles with well-controlled and distinctive shapes under similar synthetic conditions. Fig. S1a shows the cubic shell structure of AgNCs with an average particle size of about 80 nm, which was equipped with uniform morphology and favorable dispersibility, in line with the SEM results (Fig. S1b). In comparison, after Pt replace Ag, the structure of PtNFS nanoparticles was a thin layer of two-dimensional structure with a size of about 80 nm (Fig. 1a), thereby intuitively providing that PtNCs was successfully prepared.

As revealed by EDS map (Fig. 1b) that in the preparation of the PtNFs materials containing C, O, Cu, Ag and Pt elements, wherein O and part C were derived from OCT template, and a large amount of Cu was derived from copper grid. Ag and Pt elements were derived from the two-dimensional structure of the nanoflakes, and the trace amount of Ag may be due to the reduction of silver ions in solution or the deposition of silver chloride on the surface of Pt crystals. From Fig. 1c, it's extremely strong characteristic peak at 46.1° indicated that (111) crystal plane of Pt crystal low-energy crystal, namely a polypeptide specific binding or selective deposition of silver chloride crystal.[23]

FTIR analysis of PtNFs was further carried out to study the effect of OCT binding on Pt surface to control morphology. It is reported that the infrared absorption of different amide I band has a corresponding secondary structure. It can be seen from Fig. 1d that the characteristic vibration peaks of OCT still exist after the preparation of dendritic structure, the most significant difference in the characteristic peaks between PtNFs and OCT was the changes in the peak positions of O-H bonds and amide bonds, confirmed that Pt crystals and OCT are bonded by amide bonds and hydroxyl groups.[24]

Synthetic mechanism of PtNFs. The process of PtNFs synthesis and the role of polypeptides are described in detail. In order to elaborate the preparation process of the PtNFs, the sample of the solution which was not added at the initial stage of the reaction was examined for TEM. As shown in the Fig. S2, only the substitution reaction between Ag-Pt was carried out at the beginning of the

reaction, and the Pt nanoparticles were nucleated on the surface of the AgNCs without the process of alloying due to the lack of solid-solid diffusion between the Pt and the Ag. And at this point, the Pt nano-crystal nucleus does not form a definable morphology, indicating that the Pt crystal nucleus is not affected by the polypeptide located inside the AgNCs at this time. As the displacement reaction proceeds, the AgNCs is gradually disintegrated into the dispersed small-size nano-particles by the 3D structure, and the inner OCT is exposed to be combined with the Pt crystal nucleus so as to contribute to the formation of the cubic Pt crystal nucleus and the growth of the nano-flakes (Fig. 2). This further confirms the theory of the formation of the polypeptide-mediated PtNFs.

It should be taken seriously that the concentration of precursor and reaction time are crucial factors to influence the morphology of nanoparticles, which was demonstrated in regulating nanocrystal shapes. A series of reactions were performed with changing concentrations of $PtCl_4$ solution that can induce a shape transformation from octahedron to cubes (Fig. 2a-c). As shown in Fig. 2a, the nanocrystals, which were near-spherical truncated octahedron with nucleating rapidly under the concentration of 0.5 M $PtCl_4$ (10 min), and preferential adsorption of Pt (100) during growth of nuclei with cuboctahedron shape, accompanied by the different growth rates between the (111) and (100) faces, plays key role to the formation of Pt cube. With the extending the concentration of $PtCl_4$, the nanocrystals emerged prominently a growth tendency. Under the concentration of 1M $PtCl_4$, the surface of the (100) crystal of the generated

nanocrystals continuously increased, while the surface of the (111) crystal was relatively reduced, forming a nearly cubic truncated octahedral structure (Fig. 2b). Subsequently, the concentration of $PtCl_4$ was enriched to 2 mM, the representative cubic structure of PtNFs is successfully formed (Fig. 2c). Since no obvious size addition was observed during the shape evolution process, It can be believed that tetrahedral formation may be attributed to the atomic rearrangement on the surface of nanocrystals induced by the interaction between binding peptides and surface atoms, resulting in the formation of cube nanocrystals eventually.[24, 25]

Interestingly, after an hour of reaction, the shape of the nanocrystals had transformed from equably cubes to flake, and a plate-like layer of aggregated particulates was formed (Fig. 2d), illustrating that the cubic crystal without cutting angles beneficial to the anisotropic growth of amorphous nanocrystals.[26] Better yet, the morphology of resulting nano-flakes still was affected on account of enriched $PtCl_4$ concentrations but it made little difference in terms of thickness. Fig. 2d-f present that the larger the size and more aggregation of PtNFs obtained with the incremental the concentration of $PtCl_4$. This nanostructures of nano-flakes show advantages such as high specific surface, strong energy storage, excellent electrochemical activity.[27] In brief, these results further confirmed the interaction between OCT and Pt crystal to modulate surface energies of nanocrystals and guided the shape formation and transformation processes, which are likely to play a key role in the electrode performance.

Characterization and electrochemical property of the BGSs. As revealed by the TEM (Fig. 3a) and SEM (Fig. 3b), the synthesized BGSs exhibited a distinct branched structure with a solid core and plenty of edges and tips. The interaction of the core and tip plasma of the nanoparticles amplified cross-section to excite surface plasmon resonance and results in local electric field enhancement, which was stronger than a single tip or smooth structure.[28]

The electrochemical properties of BGSs were investigated by CVs experiments. As shown in Fig. 3c, the maximum currents of the oxidation peaks (78.77 mA) and reduction peaks (-126.6 mA) of BGSs were much larger than those of Pd/C catalysts, symbolizing that BGSs had significantly higher current density and mass activity. Further, Fig. 3d displays the catalytic performances of BGSs and Pd/C used for the oxidation reaction of ethanol, the electrolyte was a 1.0 M KOH solution containing 1.0 M C_2H_5OH solution. During the pre-sweep process, the current density of the BGSs was 5.5 mA cm^{-2}, which was 5.5 times that of the Pd/C catalyst (1.0 mA cm^{-2}). The good electrocatalytic activity of BGSs was attributed to its shell structure and dendritic surface, with more catalytic active sites and better electron conduction efficiency, signifying its potential as a signal enhancement material.[29]

In order to further study the durability of BGSs, 500 cyclic potential scans were performed in 1.0 M KOH solution and 1.0 M KOH 1.0 M C_2H_5OH solution in the potential range of-0.4 and 0.6V, respectively. As shown in Fig. S3a, b, BGSs

shows good stability throughout the test phase. As shown in Fig. S3b, the peak current density of the BGSs modified electrode remained 81% after 500 cycles.

In order to prove that RGO/BGSs can really improve signal amplification, we have conducted two kinds of experiments to study its amplification characteristics (a. HeLa cells/OCT/BGSs/RGO modified GCE + signal probe, b. HeLa cells/ OCT modified GCE + signal probe). The DPV curve in both cases is shown in Fig. S4. It can be seen from curve b that the change of electrochemical signal is much larger than that of curve a, which may be due to the increase of the specific surface area of BGSs/OCT layer and the increase of conductivity.

Analysis of biocompatibility. Biosafety of biosensor should be considered first in medicine applications, therefore, the biological compatibility of PtNFs was evaluated using live/dead cell staining experiments with fluorescein diacetate (FDA). First, PtNFs modified ostensibly by OCT, which was improved the biocompatibility effectively compared with pure metal nanoparticles, was used for cell staining and no obvious toxicity was detected in the range of 0-100 μg mL^{-1} under the incubating for 24 h, verifying the safety of the biosensor (Fig. 4a-c). Meanwhile, the incubation time of the nanoparticles (50 μg mL^{-1}, 100 μg mL^{-1}) was further extended to 48 h, the fluorescence intensity of the HeLa cells made little difference significantly, indicating that the OCT modified PtNFs still possessed low toxicity (Fig. 4d-f). Subsequently, cell activity was detected through the standard MTT assay, the cell viability of HeLa cells incubated with (Fig. 4g) PtNFs or (Fig. 4h) BGSs demonstrated good biocompatibility of

electrode materials. In addition, the biosafety of BGSs has been confirmed in previous reports.[22] These results revealed that remarkable biocompatibility and low toxicity support the PtNFs as an excellent candidate for biological sensing applications.

Characterization of the modified electrodes. GCE was modified by layer-by-layer assembly technique, in which RGO was used as a substrate material to amplify the specific surface area of GCE to improve the conductivity of the electrode, while enhancing the transfer ability of electrons to the electrode surface and for depositing dendritic gold nanoparticles. Similarly, BGSs were used to enhance electron conduction and amplify signal transmission and OCT was used to accurately identify of SSTRs and capture HeLa cells.

Fig. 5a shows the CV curves for various modified electrodes such as bare GCE, GCE/RGO/BGSs and GCE/RGO/BGSs/Lan-HeLa in N_2 saturated PBS at a scan rate of 50 mV/s. The bare GCE, GCE/RGO were shown minuscule redox behavior with oxidation peak potential (EPA) of about 0.208 V, 0.204 V, respectively. Meanwhile, the CV curve of GCE/RGO/BGSs shows a pair of well-defined redox peaks appeared under the action of $[Fe(CN)_6]^{-3/-4}$ redox coupling, which arose due to the ultra-high specific surface area of RGO/BGSs for excellent electrical conductivity and the formation of synergistic effect of bimetals with RGO.[30, 31] As expected, the current intensity decreased after the OCT modified electrode, expressing that the OCT molecules had been successfully immobilized on the electrode surface, and the current intensity was further

decreased after the electrode was incubated with HeLa cells, signifying that OCT can successfully capture tumor cells and hinder the transfer of electrons between the electrodes. The decrease in current intensity was consistent with the fact that the protein hydrophobic layer insulates the conductive carrier. In summary, the modification of cyclic voltammetric peak current of GCE modified by different materials confirms that it was feasible to modify GCE by layer assembly technique.[32]

The semi-circular diameter of the Nyquist chart corresponds to the charge transfer resistance (Rct), and the change in Rct (Fig. S5) was attributed to the different modifications of the electrodes. As is shown in Fig. 5b, the bare GCE produced an EIS, which initially indicated a large curvature radius dimension with relatively large resistance. when the GCE/RGO and GCE/RGO/BGSs were tested, the EIS initially produced a strongly curved profile, which then effectively straightened out, because the BGS is good electron conductor.[33] However, after the surface of the electrode is modified by OCT, ESI curve presents a definite, significant curvature followed by essentially a linear plot, suggesting that the electron transfer was hindered by the negative charge of the polypeptide molecule, which caused the intensification of arc radius and resistance.[34] The resistance was further intensified after incubation of the RGO/BGSs/OCT modified electrode and cells, producing an essentially large radius of EIS plot with initial curvature, the plot effectively signified that successful modification of GCE had been achieved by layer-by-layer assembly, and HeLa cells can be successfully captured.[35] It's

worth mentioning that the results were consistent with those from the CV works described above, which similarly proved that it can be used in the construction of electrochemical biosensors to detect tumor cells.

Conditions optimization. The proposed cell sensor depends on the OCT immobilized on the surface of the electrode. So the concentration of OCT (0.2-0.7 mM) was optimized by DPV experiment (Fig. S6a). When the concentration of OCT reaches 0.5 mM, the maximum current intensity is achieved. Therefore, the optimum concentration of OCT is 0.5 mM.

The concentration of Signal probe is also a very important condition for the practicability of the sensor. The current response increases sharply with the increase of the concentration of signal probe, and reaches a platform at the concentration of 10mM (Fig. S6b). Then, when the concentration exceeds the current intensity of 10 mM, the current intensity does not change much. These results indicate that the maximum peak current can be obtained when the concentration of signal probe is 10 mM.

Electrochemical sensing of HeLa on GCE/RGO/BGSs. Ultimately, the signal amplification strategy of the constructed biosensor was further proved by DPV experiments and the tumor cells were quantitatively detected.[36] Based on the constructed electrochemical biosensor, we applied the GCE/RGO/BGSs/OCT to the sensing of HeLa by varying concentrations from 10 to 1×10^6 cells mL^{-1} in 0.01 M PBS (pH 7.4) and human whole blood samples. Cancer cells were captured by electrostatic adsorbed OCT through specific binding. Then the prepared Pt signal

probe was introduced into DPV detection, which also bound to somatostatin receptor on the surface of HeLa cells to form sandwich structure on the electrode. A large number of Pt signal probe adsorbed on the cell surface catalyzed the reduction of H_2O_2, thus increasing the reduction peak current of the electrode. The probe based on appropriate concentration can make the cell concentration and current intensity show a certain linear relationship. Fig. 5c shows that H_2O_2 reduction had a good concentration dependence on HeLa cells. As the concentration of HeLa cells increased, the current responsiveness also increased. In the range from 10 to 1×10^6 cells mL^{-1} HeLa cells, the current response had a good linear relationship with the logarithm of HeLa cell concentration (Fig. 5d). The linear regression equation is Y=25.25Log[C]+4.2, and the linear relationship coefficient is 0.9998 (n=6), where Y is the peak current of the electrochemical cell sensing and C is the concentration of HeLa cells. Under the condition of signal-to-noise ratio of 3, the LOD of HeLa cells can be calculated from the calibration curve to be 2 cells mL^{-1}. Compared with the previous methods (Table S1), the constructed sensor showed a lower LOD and a wider linear range, indicating that the signal amplification based on composite probe of PtNFs/OCT and electrode modification of RGO/BGS/OCT by the layered assembly can achieve the tracking and monitoring of HeLa cells, which very promising for clinical applications.

Cell selectivity of GCE/RGO/BGSs/OCT. It is necessary to use different cell lines to evaluate the specificity of the developed immunosensors. Under the same

experimental conditions, three different kinds of cells were added to human serum. The control group was treated with the same concentration of tumor cells (1×10^6 cells mL^{-1}) in PBS buffer. The DPV analysis of different types of tumor cells showed that the response from 293T cells could be negligible as shown in the Fig. S7. The detection of HeLa, A549 cells has a high current response, indicating that the developed immunosensor has high specificity for the recognition and detection of tumor cells. The current intensity of A549 is slightly higher because of the higher expression of SSTRs. The DPV current of clinical samples with different cells was slightly lower than that of PBS samples containing the same number of cells, which may be due to the nonspecific adsorption of proteins in blood samples, but there was no significant difference. The results show that the method has excellent cancer cell selectivity in complex actual samples.

Reproducibility and stability of the GCE/RGO/BGSs. To evaluate the reproducibility and potential application value of this biosensor in complex real samples, different concentrations of HeLa cells are added to the blood sample to calculate the recovery rate of the sensor. Results as shown in Table S2, the RSD values of the biosensors with different cell concentrations were calculated as 2.76%, 4.23% and 2.95%, respectively, indicating that the biosensors had good reproducibility. In addition, the value of the recovery rate indicates that the method has a good applicability to the analysis of cancer cells. To estimate the stability of the GCE/RGO/OCT-BGSs, as shown in Fig. S8, the sensor (fresh or which was stored in a refrigerator at 4°C for two weeks) whose initial current

response was 92% active compared to the newly prepared electrode, symbolizing that the constructed electrochemical biosensor had good stability , which was attributable the good stability of electrochemical devices in each part.

CONCLUSIONS

In this study, an ultrasensitive sandwich electrochemical biosensor based on BGSs/OCT and PtNFs/OCT nanocomposites was designed, which was used for detection of tumor-specific markers to evaluate tumor cells. Unique highly BGS and two-dimensional thin films were prepared under mild conditions. PtNFs are used to enhance the specific surface area of GCE to improve the conductivity of the electrode. OCT not only serves as a bio-template for metal synthesis, but also specifically recognizes tumor surface markers, so as to rapidly and sensitively determine HeLa cells quantitatively. This experiment demonstrates that PtNFs/OCT is an ideal biocompatible nanomaterial with good electron transfer capability and significantly amplifies the current signal when used as a signal probe. Based on the above advantages, the electrochemical biosensor prepared this time has higher sensitivity and wider detection range than other methods, and achieves signal enhancement effect, reducing the LOD to 2 cells mL^{-1} for cancer. The high specificity and sensitivity of the biosensor will be beneficial for early diagnosis of tumor and evaluation of therapeutic effect. Moreover, this strategy can easily be extended to varieties types of tumors.

ASSOCIATED CONTENT

Supporting Information

TEM images of the silver nanocage, TEM images of the initial phase of ag-pt reaction, potential scanning of the BGS modified electrode, DPV response under different modification conditions, current response to different OCT and probe concentrations, and electrochemical response to different cell lines.

ACKNOWLEDGMENTS

This work was supported by the National Natural Science Foundation (No. 21776238, 21476190, 31801198), the Hebei province key basic research Foundation (No. 15961301D), Hebei education department key project (No. ZD2017084).

REFERENCES

[1] B.E. Rapp, F.J. Gruhl, K. Länge, Biosensors with label-free detection designed for diagnostic applications, Anal. Bioanal. Chem. 398 (2010) 2403-2412.

[2] T. Guan, X. Wang, D. Li, Y. Zhang, Y. He, L. Shi, Y. Liu, Y. Yang, Y. Xu, R. Cui, Determination of tumor marker carcinoembryonic antigen with biosensor based on optical quantum weak measurements, Sensors 18 (2018) 1550.

[3] Y. Tian, X. Chen, L. Shuang, L. Ying, S. Liu, Affinity binding-induced Hg^{2+} releasing and quantum dot doping for general, label-free, and homogenous fluorescence protein assay, ACS Sens. 3 (2018) 1401-1408.

[4] T. Florio, Molecular mechanisms of the antiproliferative activity of somatostatin receptors (SSTRs) in neuroendocrine tumors, Front. Biosci. 13 (2008) 822-840.

[5] J. Schäfer, H. Baumeister, W. Meyerhof, R. Nehring, D. Richter, Characterization of cloned somatostatin receptor subtypes Localization of rat SSTRs in gastrointestinal tissues, SSTR1 gene promoter studies, and mutational analyses of SSTR3, Ann. N.Y. Acad. Sci. 805 (2010) 601-606.

[6] T. Yin, Q. Wu, L. Wang, L. Yin, J. Zhou, M. Huo, Well-defined redox-sensitive polyethene glycol-Paclitaxel prodrug conjugate for tumor-specific delivery of paclitaxel using octreotide for tumor targeting, Mol. Pharmaceutics 12 (2015) 3020-3031.

[7] Q. Yang, X. Wu, H. Peng, L. Fu, X. Song, J. Li, H. Xiong, L. Chen, Q. Yang, X. Wu, Simultaneous phase-inversion and imprinting based sensor for highly sensitive and selective detection of bisphenol A, Talanta 176 (2017) 595-603.

[8] A.H. Nguyen, J. Sang, Detection and amplification of dual bio-signatures of circulating tumor DNA, Biosens. Bioelectron. 67 (2015) 443-449.

[9] Y. Iwase, Y. Maitani, Octreotide-targeted liposomes loaded with CPT-11 enhanced cytotoxicity for the treatment of medullary thyroid carcinoma, Mol. Pharmaceutics 8 (2011) 330-337.

[10] M. Hasanzadeh, N. Shadjou, M. Guardia, Recent advances in nanostructures and nanocrystals as signal-amplification elements in electrochemical cytosensing, TrAC, Trends Anal. Chem. 72 (2015) 123-140.

[11] X. Zhuang, D. Chen, S. Zhang, F. Luan, L. Chen, Reduced graphene oxide functionalized with a CoS_2/ionic liquid composite and decorated with gold nanoparticles for voltammetric sensing of dopamine, Microchimica Acta 185(3) (2018) 166.

[12] X. Zhuang, D. Chen, S. Wang, H. Liu, L.J.S. Chen, Manganese dioxide nanosheet-decorated ionic liquid-functionalized graphene for electrochemical theophylline biosensing, Sens. Actuators, B Chem. 251 (2017), 185-191.

[13] L. Li-Min, L. Hong-Bo, Q. Fengli, Z. Xiao-Bing, S. Guo-Li, Y. Ru-Qin, In situ synthesis of palladium nanoparticle-graphene nanohybrids and their application in nonenzymatic glucose biosensors, Biosens. Bioelectron. 26 (2011) 3500-3504.

[14] J. Hao, L. Ji, K. Wu, N. Yang, Electrochemistry of ZnO@reduced graphene oxides, Carbon 130 (2018) 480-486.

[15] C. Wang, F. Jiang, R. Yue, H. Wang, Y. Du, Enhanced photo-electrocatalytic performance of Pt/RGO/TiO_2 on carbon fiber towards methanol oxidation in alkaline media, J. Solid State Electrochem. 18 (2014) 515-522.

[16] Y. Xue, H. Zhao, Z. Wu, X. Li, Y. He, Z. Yuan, The comparison of different gold nanoparticles/graphene nanosheets hybrid nanocomposites in electrochemical performance and the construction of a sensitive uric acid electrochemical sensor with novel hybrid nanocomposites, Biosens. Bioelectron. 29 (2011) 102-108.

[17] W. Yafeng, X. Peng, K. Yuejun, K.M. Hui, Highly specific and ultrasensitive graphene-enhanced electrochemical detection of low-abundance tumor cells using silica nanoparticles coated with antibody-conjugated quantum dots, Anal. Chem. 85 (2013) 3166-3173.

[18] C.Y. Chiu, Y. Li, L. Ruan, X. Ye, C.B. Murray, Y. Huang, Platinum nanocrystals selectively shaped using facet-specific peptide sequences, Nat. Chem. 3 (2011) 393-399.

[19] D. Chen, X. Zhuang, Z. Jian, Y. Zheng, L. Hua, L. Preparation of highly sensitive Pt nanoparticles-carbon quantum dots/ionic liquid functionalized graphene oxide nanocomposites and application for H_2O_2 Detection, Sens. Actuators, B Chem. 255 (2018) 1500-1506.

[20] S. Liu, J. Wang, J. Zeng, J. Ou, Z. Li, X. Liu, S. Yang, “Green” electrochemical synthesis of Pt/graphene sheet nanocomposite film and its electrocatalytic property, J. Power Sources 195 (2010) 4628-4633.

[21] K. Bian, X. Zhang, L. Kai, Y. Tian, H. Liu, N. Kang, W. Cao, D Gao, Peptide-Directed Hierarchical Mineralized Silver Nanocages for Anti-Tumor Photothermal Therapy, . ACS Sustainable Chem. Eng. 6 (2018) 7575-7588

[22] K. Bian, X. Zhang, M. Yang, L. Luo, L. Li, Y. He, C. Cong, X. Li, R. Zhu, D. Gao, Dual-template cascade synthesis of highly multi-branched Au nanoshells with ultrastrong NIR absorption and efficient photothermal therapeutic intervention, J. Mater. Chem. B 7 (2019) 598-610.

[23] Y. Sun, Controlled synthesis of colloidal silver nanoparticles in organic solutions: Empirical rules for nucleation engineering, Chem. Soc. Rev. 42 (2013) 2497-2511.

[24] R. Diaz-Espinoza, E. Nova, O, Monasterio, Overcoming electrostatic

repulsions during amyloid assembly: Effect of pH and interaction with divalent metals using model peptides, Arch. Biochem. Biophys. 621 (2017) 46-53.

[25] Y. Zhao, Y. Wei, C. Chen, J. Wang, L. Zhang, X. Hai, Rational design and self-assembly of short amphiphilic peptides and applications, Curr. Opin. Colloid Interface Sci. 35 (2018) 112-113.

[26] M. Miyake, K. Miyabayashi, Shape and size controlled Pt nanocrystals as novel model catalysts, Catal. Surv. Asia 16 (2012) 1-13.

[27] K. Thangavelu, N. Raja, S.M. Chen, W. Liao, Nanomolar electrochemical detection of caffeic acid in fortified wine samples based on gold/palladium nanoparticles decorated graphene flakes (Au/PdNPs-GRF), J Colloid Interface Sci 501 (2017) 77-85.

[28] J. Xie, J.Y. Lee, D. Wang, Seedless, surfactantless, high-yield synthesis of branched gold nanocrystals in HEPES buffer solution, Chem. Mater. 19 (2007) 2823-2830.

[29] S. Thangavel, R. Ramaraj, Electroless synthesis of multibranched gold nanostructures encapsulated by poly (o-phenylenediamine) in Nafion, J. Colloid Interface Sci. 355 (2011) 293-299.

[30] F. Li, Y. Guo, L. Yue, H. Qiu, X. Sun, W. Wei, L. Yu, J. Gao, Fabrication of Pt–Cu/RGO hybrids and their electrochemical performance for the oxidation of methanol and formic acid in acid media, Carbon 64 (2013) 11-19.

[31] J. Hai-Jun, W. Xiao-Lan, P. Smrutiranjan, W. Ke, S. Masahiro, W. JöRg, Nanoporous Au-Pt alloys as large strain electrochemical actuators, Nano Lett. 10 (2010) 187-194.

[32] H. Song, Y. Ni, S. Kokot, A novel electrochemical biosensor based on the hemin-graphene nano-sheets and gold nano-particles hybrid film for the analysis of hydrogen peroxide, Anal. Chim. Acta 788 (2013) 24-31.

[33] J. Zhu, C. Sun, D. Xue, Electrochemical route to branched gold nanostructures, J. Alloys Compd. 639 (2015) 27-35..

[34] X. Hou, M. Zhang, J. Wang, S. Hu, X. Liu, Z. Shao, High yield and low-cost ball milling synthesis of nano-flake Si@SiO_2 with small crystalline grains and abundant grain boundaries as a superior anode for Li-ion batteries, J. Alloys Compd. 639 (2015) 27-35.

[35] S. Lee, H. Kim, H. Jung, Interfacial generation of plates assembled with α-Fe_2O_3 nano-flakes for electrochemical capacitors, J. Electroanal. Chem. 770 (2016) 44-49.

[36] J. Zhang, P. Chen, X. Wu, J. Chen, L. Xu, G. Chen, F. Fu, A signal-on electrochemiluminescence aptamer biosensor for the detection of ultratrace thrombin based on junction-probe, Biosens. Bioelectron. 26 (2011) 2645-2650.

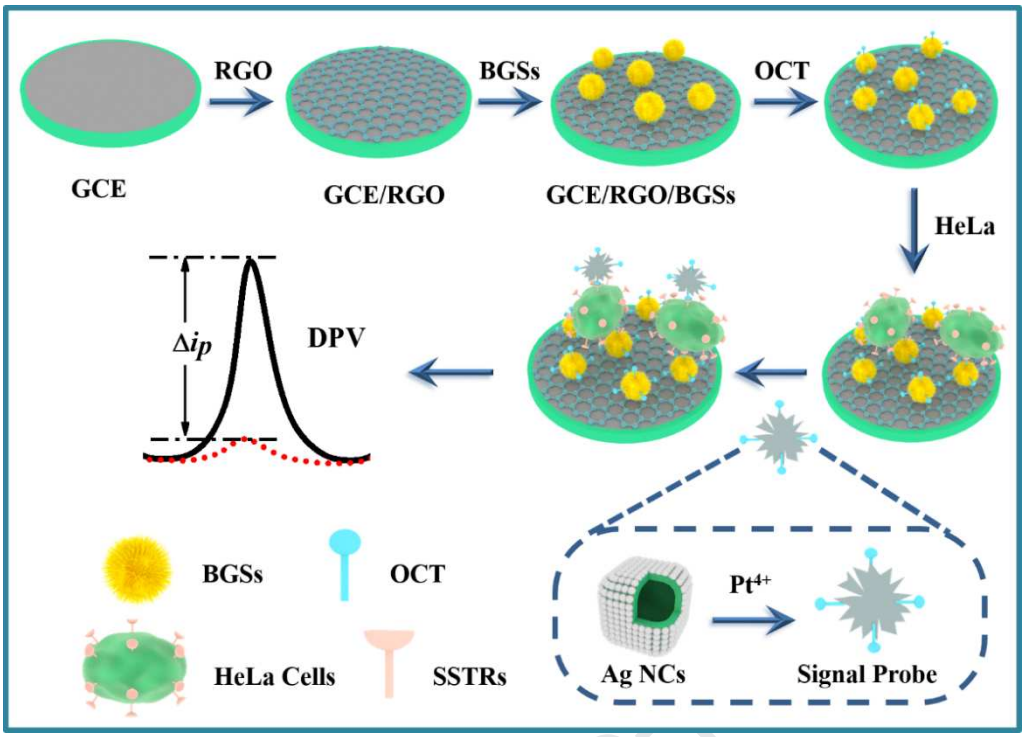

Scheme 1. Schematic illustration of sandwich-like electrochemical geometry for the cytosensing of HeLa cells.

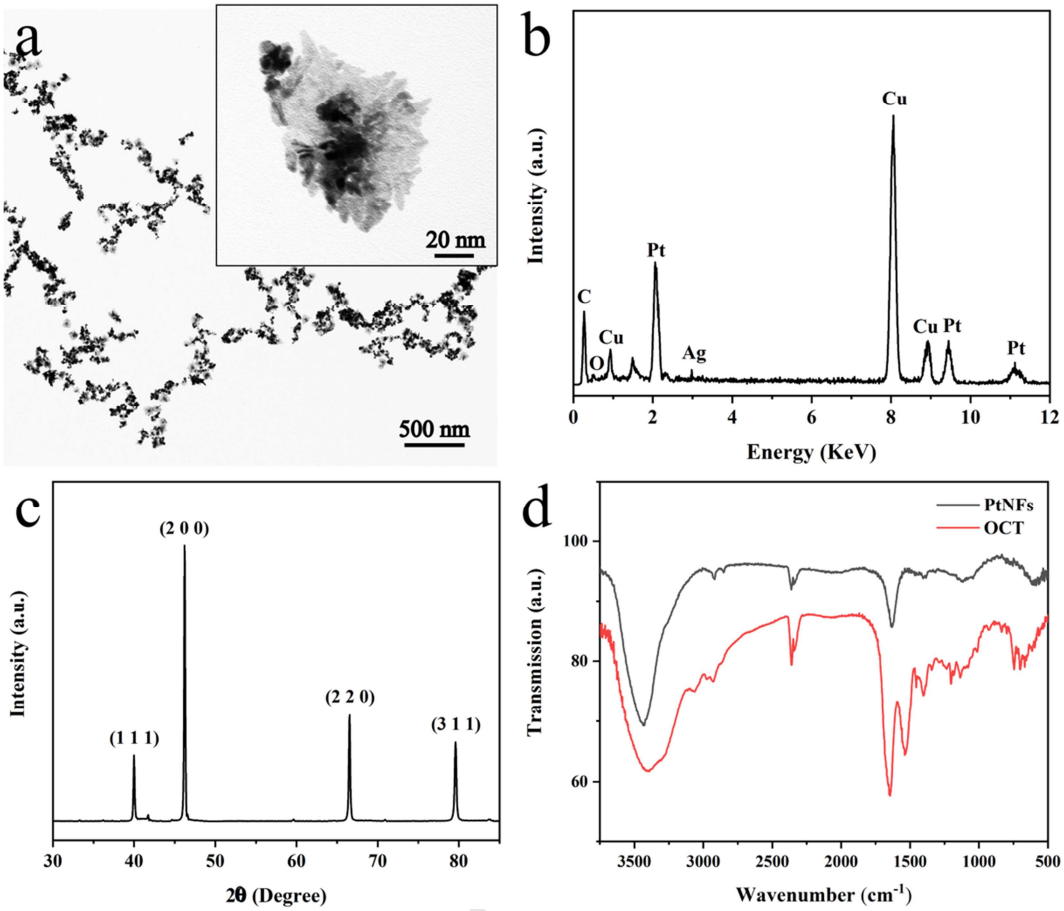

Fig. 1. (a) TEM image of PtNFs; (b) EDS image, (c) XRD patterns and (d) FT-IR spectra of PtNFs.

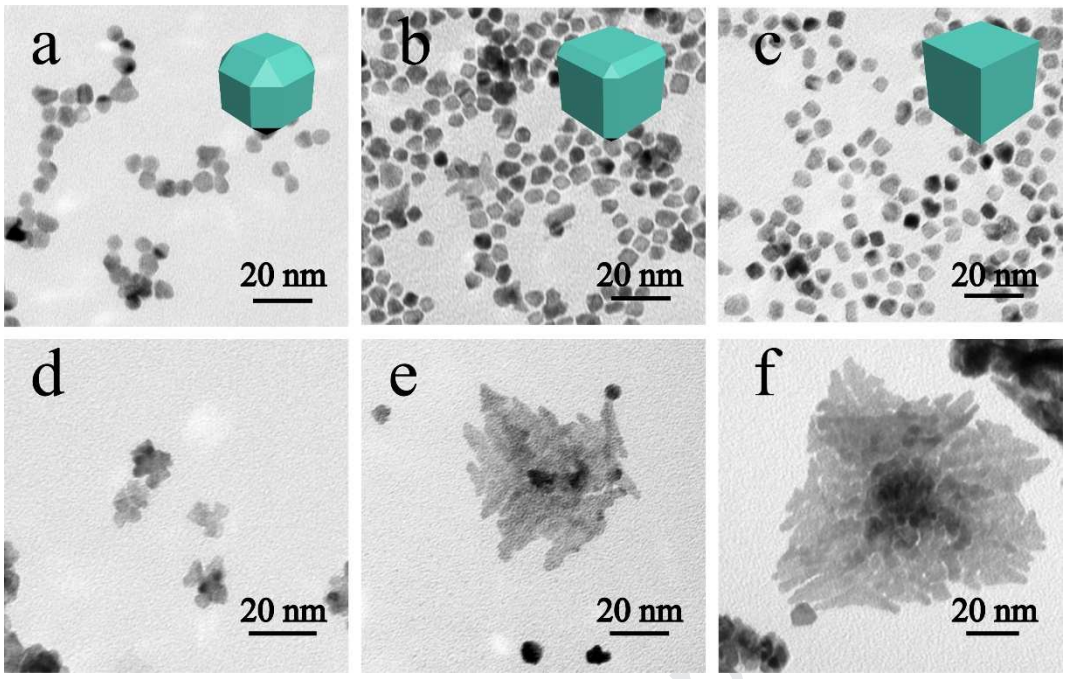

Fig. 2. TEM images of nanocrystals obtained at different concentrations of $PtCl_4$ ((a) 0.5 mM, (b) 1 mM, (c) 2 mM) and at different reaction times ((a-c) 10 min, (d-f) 1 h).

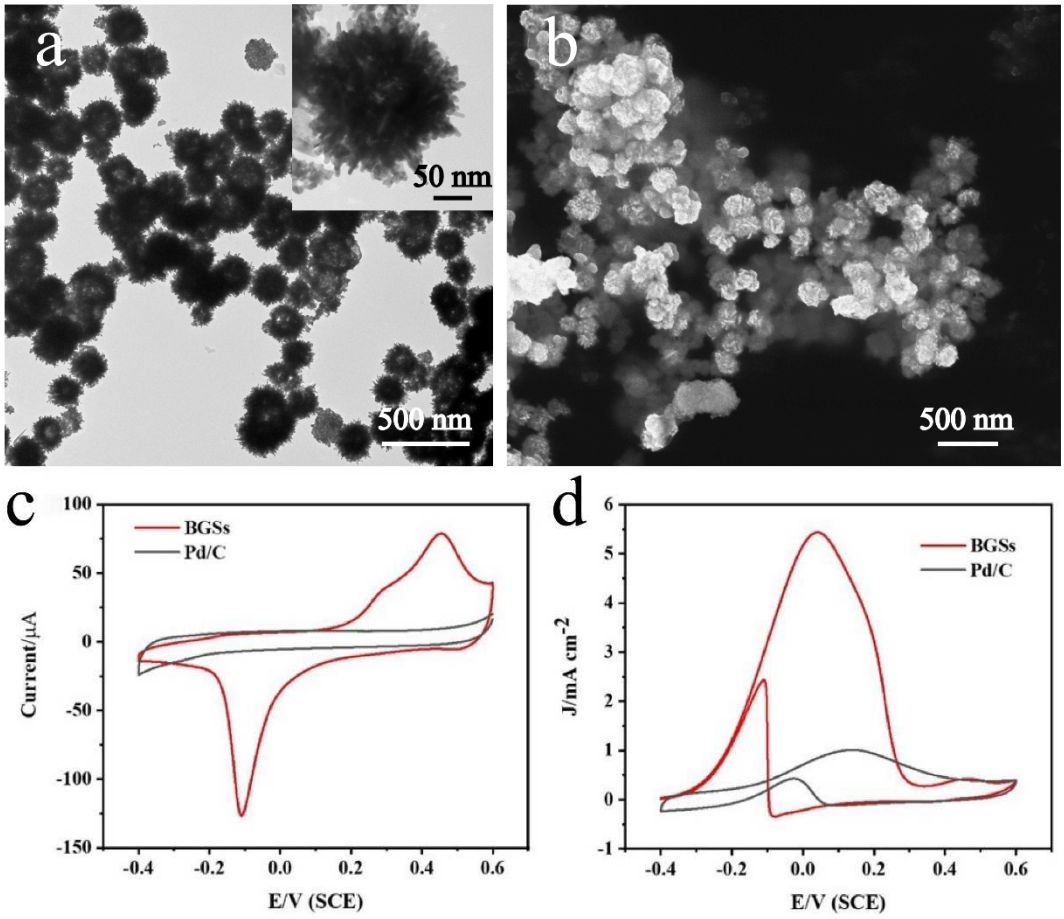

Fig. 3 (a) TEM images and (b) SEM image of GCEs; CV curves of commercial Pd/C and BGSs modified electrodes in the (c) 1.0 M KOH solution and (d) 1.0 M KOH + 1.0 M C_2H_5OH solution.

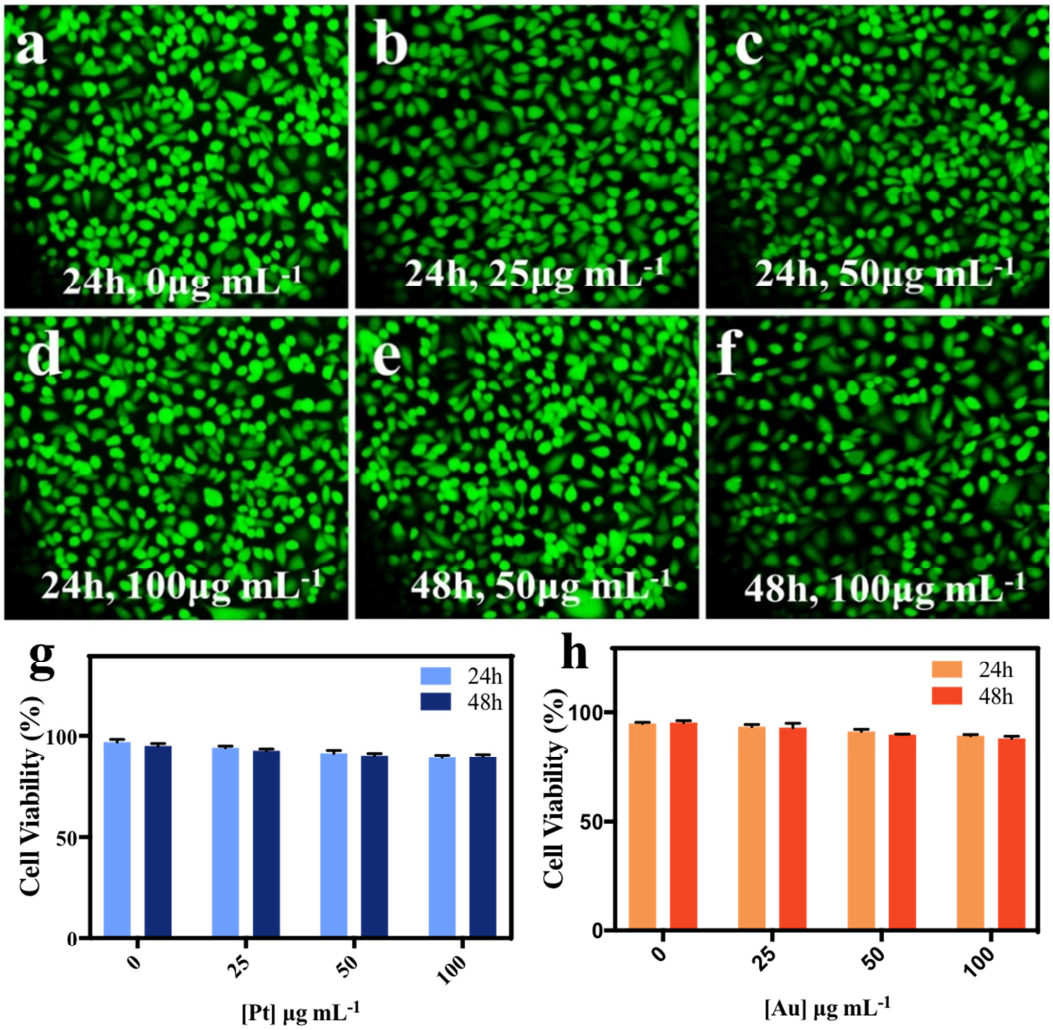

Fig. 4 Fluorescent images of HeLa cells incubated with PtNFs at (a) 0, (b) 25, (c) 50, (d) 100 μg mL^{-1} of PtNFs for 24 h or incubated with PtNFs at (e) 50, (f) 100 μg mL^{-1} for 48 h. Cell viability of HeLa cells incubated with (g) Pt NFs or (h) BGSs at 0, 25, 50, 100 μg mL^{-1} of metal.

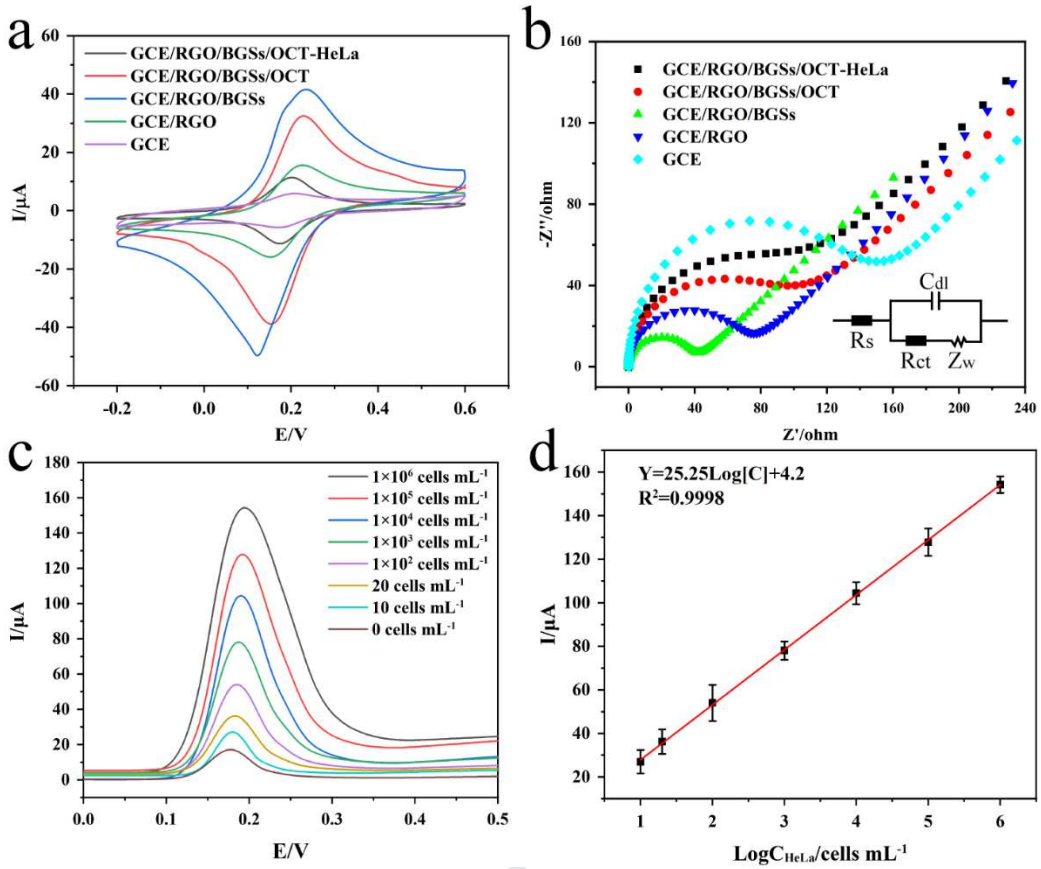

Fig. 5 (a) CVs and (b) Nyquist plots obtained from different electrodes in PBS solution containing 5 mM $[Fe(CN)_6]^{-3/-4}$ and 0.1 M KCl; (c) DPV responses of the electrochemical biosensor incubated with HeLa cells of different concentrations in 0.01 M PBS. (d) Calibration curve of the electrochemical biosensor for HeLa cells.

Highlights

1. For the first time, octreotide was used to target somatostatin receptors to achieve effective detection of tumor cells.
2. Platinum nano-flakes were prepared by green and simple methods for the construction of electrochemical biosensors.
3. The electrochemical signal of the biosensor is significantly amplified based on the unique morphology of the platinum nanosheet.
4. Realize low detection limit signal monitoring by rationally utilizing the characteristics of various materials.